

1 **Deglaciation of the Caucasus Mountains, Russia / Georgia, in the 21st century observed**
2 **with ASTER satellite imagery and aerial photography**

3

4 Maria Shahgedanova¹, Gennady Nosenko², Stanislav Kutuzov^{1,2}, Oksana Rototaeva² and Tatyana
5 Khromova²

6 ¹ Department of Geography and Environmental Science and Walker Institute for Climate System
7 Research, University of Reading, Whiteknights, Reading RG6 6AB, UK.

8 ² Laboratory of Glaciology, Institute of Geography, Russian Academy of Sciences, 29
9 Staromonetny Pereulok, Moscow, 119017, Russia. Tel: +7 499 1259011; Fax: +7 495 9590033;
10 Correspondence to: M. Shahgedanova (m.shahgedanova@reading.ac.uk)

11

12 **Abstract**

13 Changes in map area of 498 glaciers located on the Main Caucasus Ridge (MCR) and on Mt.
14 Elbrus in the Greater Caucasus Mountains (Russia and Georgia) were assessed using
15 multispectral ASTER and panchromatic Landsat imagery with 15 m spatial resolution from
16 1999-2001 and 2010-2012. Changes in recession rates of glacier snouts between 1987-2001 and
17 2001-2010 were investigated using aerial photography and ASTER imagery for a sub-sample of
18 44 glaciers. In total, glacier area declined by $4.7 \pm 1.6\%$ or 19.24 km^2 from 407.35 km^2 to 388.11 km^2 . Glaciers located in the central and western MCR lost 13.4 km^2 ($4.6 \pm 1.8\%$) in total or 8.56 km^2 ($5.0 \pm 1.8\%$) and 4.87 km^2 ($4.1 \pm 1.9\%$) respectively. Glaciers on Mt. Elbrus, although located
21 at higher elevations, lost 5.8 km^2 ($4.9 \pm 0.7\%$) of their total area. The recession rates of valley
22 glacier terminus increased between 1987 - 2000/01 and 2000/01 - 2010 from $3.8 \pm 0.8 \text{ m a}^{-1}$,
23 $3.2 \pm 0.9 \text{ m a}^{-1}$ and $8.3 \pm 0.8 \text{ m a}^{-1}$ to $11.9 \pm 1.1 \text{ m a}^{-1}$, $8.7 \pm 1.1 \text{ m a}^{-1}$ and $14.1 \pm 1.1 \text{ m a}^{-1}$ in the

24 central and western MCR and on Mt. Elbrus respectively. The highest rate of increase in glacier
25 termini retreat was registered on the southern slope of the central MCR where it has tripled. A
26 positive trend in summer temperatures forced glacier recession and strong positive temperature
27 anomalies of 1998, 2006, and 2010 contributed to the enhanced loss of ice. An increase in
28 accumulation season precipitation observed in the northern MCR since the mid-1980s has not
29 compensated for the effects of summer warming while the negative precipitation anomalies,
30 observed on the south slope of the central MCR in the 1990s, resulted in stronger glacier
31 wastage.

32

33 **1 Introduction**

34 Shrinkage of mountain glaciers in response to the observed climatic warming has been
35 documented worldwide. The 1990s and 2000s were the warmest decades in the 150-year
36 instrumental record (IPCC, 2013; see their Fig. 2.19), with global surface temperature anomalies
37 of 0.24°C and 0.44°C above the 1961-1990 mean respectively
38 (www.metoffice.gov.uk/research/monitoring/climate/surface-temperature). Mountain glaciers are
39 sensitive indicators of climatic change at the decadal time scale (Hoelzle et al., 2003) and
40 acceleration in their area and volume reduction in the 1990s has been reported for many regions
41 (Dyurgerov and Meier, 2000; Zemp et al., 2009). The contribution of glaciers and ice caps
42 (excluding Antarctica and Greenland) to the global sea level budget increased from 0.67 ± 0.03
43 mm a^{-1} in 1972-2008 to $0.99 \pm 0.04 \text{ mm a}^{-1}$ in 1998-2008, in line with intensifying climatic
44 warming and glacier melt (Church et al., 2012).

45 Remote sensing is an established way of monitoring changes in glacier area and positions of
46 glacier snouts. To date, most assessments have been conducted using multispectral Landsat

47 Thematic Mapper (TM) and Enhanced Thematic Mapper Plus (ETM+) imagery, with 30 m
48 horizontal resolution available since 1982 and 1999 respectively, and Advanced Spaceborne
49 Thermal Emission and Reflection Radiometer (ASTER) imagery with 15 m resolution available
50 since 2000. Together with historical aerial photographs and maps, this imagery enabled
51 assessments at time steps of 20-50 years during which magnitude of glacier change significantly
52 exceeded measurement errors. Various studies that used Landsat imagery reported measurement
53 errors from about 3-5% of single-glacier area change for clear ice (with larger errors for smaller
54 glaciers) to over 10% for debris-covered glaciers or those whose outlines merge with snow fields
55 (e.g. Paul and Andreassen, 2009; Andreassen et al., 2008; Bhambri et al., 2011). For this reason,
56 assessments at shorter intervals in most regions required data from repeated aerial surveys or
57 finer-resolution satellite imagery whose spatial extent and availability are limited (e.g. Hall et al.,
58 2003). Now, when high-resolution multispectral ASTER imagery has been available for more
59 than a decade, its consistent use should significantly reduce uncertainties in measurements of
60 glacier change and enable assessments at decadal intervals over wider regions.

61 One of the main centres of mountain glaciation in Europe is the Greater Caucasus Mountains
62 located between the Black and Caspian Seas in the densely populated south-western Russia and
63 Georgia (Fig. 1). Few studies of the Caucasus glaciers have examined large samples using
64 consistent methods and data. In the Russian-language literature, the most detailed assessments
65 are those by Panov (1993) and Yefremov et al. (2007) based predominantly on repeated field
66 measurements of positions of glacier termini in the Main (Glavny) Caucasus Ridge (MCR). In
67 the English-language literature, Stokes et al. (2006) examined changes in termini positions of
68 113 glaciers in the central Greater Caucasus between 1985 and 2000 using satellite imagery.
69 Panov's (1993) analysis of the field measurements and data derived from analysis of historical

maps showed that in the period between 1933 and 1965/70 glacier termini in the MCR retreated at an average rate of 12.3 m a^{-1} while in the period between 1965/70 and 1986/89 the recession slowed down to 6.1 m a^{-1} . In the former assessment period, glaciers of the northern and southern slopes retreated at the same rate while in the latter period, the retreat rate of 8.9 m a^{-1} observed on the southern slope exceeded the retreat rate of 4.8 m a^{-1} observed on the northern slope. Stokes et al. (2006) reported average glacier termini recession rates of 8 m a^{-1} between 1985 and 2000. From this assessment, they inferred a total loss of bare ice area of about 10% but the study did not assess changes in areas of individual glaciers. Yefremov et al. (2007) reported similar results based on field measurements. Both Stokes et al. (2006) and Yefremov et al. (2007) reported acceleration of glacier retreat in the 1990s although Yefremov et al. (2007) stressed equally high recession rates in the mid-20th Century and slow down in glacier retreat between 1965 and 1985 in line with the earlier work by Panov (1993).

Other studies focused on changes in area and fluctuation of termini of individual or small samples of glaciers. Popovnin and Petrakov (2005) provided a detailed history of shrinkage of Djankuat Glacier in the central sector of the MCR between 1968 and 1999 reporting 9% (0.29 a^{-1}) shrinkage. Kutuzov et al. (2012) examined changes in Marukh Glacier located in the western MCR showing that area reduction was similar at 17% between 1945 and 2011 (0.25 a^{-1}). Bushueva and Solomina (2012) examined recession of Kaskatash Glacier in the central MCR showing acceleration of its snout retreat rate from 1.8 m a^{-1} between 1971 and 1987 to 7.5 m a^{-1} between 1987 and 2008. More recently, changes in lengths of seven glaciers in the central greater Caucasus over the last 200 years were analysed showing that over the period these glaciers retreated with the exception of 1910-1920s and 1960-1980s, and that the rate of retreat increased since the 1990s (Lerclerq et al., 2014).

93 Changes in glacierized area on Mt. Elbrus, the largest glacierized massif in the Caucasus (Fig.
94 1), were examined by Zolotarev and Kharkovets (2007) who reported glacier shrinkage between
95 1957 and 1997. More recently, Zolotarev and Kharkovets (2012) extended these assessments to
96 2007 using data from field measurements, aerial photography and high-resolution Cartosat-1
97 imagery. According to their assessments, the total glacierized area on Mt. Elbrus declined from
98 132.51 km² in 1957 to 120.03 km² in 2007. Glacierized area declined by 0.22 km² a⁻¹ between
99 1957 and 1979, by 0.16 km² a⁻¹ between 1979 and 1997, and by 0.45 km² a⁻¹ between 1997 and
100 2007. Another assessment of glacier change on Mt. Elbrus was published by Holobaca (2013)
101 reporting area change of 9.1% between 1985 and 2007 from Landsat TM imager.

102 Continuous observations of glacier mass balance are conducted at two reference glaciers,
103 Djankuat and Garabashi (WGMS, 2013). Strong reductions in cumulative mass balance were
104 registered at both since 1995 providing further evidence of glacier wastage (Popovnin, 2000;
105 Popovnin and Petrakov, 2005; Shahgedanova et al., 2005; 2007; Rototaeva et al., 2006; Dolgova
106 et al., 2013).

107 While published assessments suggest that glaciers in the Greater Caucasus are retreating and
108 rates of retreat have accelerated at the end of the 20th century, reliable large-scale assessments of
109 changes in map areas of glaciers are not available with the exception of those by Zolotarev and
110 Kharkovets (2007; 2012) for Mt. Elbrus.

111 This paper has two objectives: (i) to quantify changes in glacier map area in the central and
112 western sectors of the Greater Caucasus Mountains between 1999/2001 and 2010/2012 using
113 ASTER imagery (or, where not available, 15-m resolution panchromatic Landsat imagery) in
114 line with the requirements of the Global Land Ice Measurements from Space (GLIMS) project
115 (<http://www.glims.org/>) and (ii) to assess changes in glacier retreat rates from the end of the 20th

116 Century to the end of the first decade of the 21st century using aerial photographs from 1987 and
117 ASTER imagery for a sub-sample of valley glaciers. Glacier snout recession is a more sensitive
118 indicator of changes at decadal time scale than area change (Hoelzle et al., 2003; Koblet et al.,
119 2010; Bhambri et al., 2012; Leclerq and Oerlemans, 2012; Leclerq et al., 2014) especially for the
120 large glacierized massifs such as Mt. Elbrus. Valley glaciers were selected for the assessment
121 because they exhibit the clearest climatic signal, being less dependent on avalanche nourishment
122 and topography than other types of glaciers (e.g. Shahgedanova et al., 2012). In this study, we
123 have chosen not to use earlier Corona imagery (used by Stokes et al. (2006)) because
124 measurement errors are potentially comparable with the derived signal over decadal intervals.
125 Nor do we analyse data from the Catalogue of Glaciers of the USSR and the World Glacier
126 Inventory (WGI) because our preliminary assessments indicated considerable uncertainties in
127 their measurements.

128

129 **2 Study region**

130 According to the Catalogue of Glaciers of the USSR (Panov and Kravtsova, 1967; Borovik and
131 Kravtsova, 1970; Maruashvili et al., 1975) and the World Glacier Inventory (WGI), the Greater
132 Caucasus accommodated over 2000 glaciers with a combined area of approximately 1600 km² in
133 the 1960s-1980s (http://nsidc.org/data/glacier_inventory/). Very close results were obtained by
134 Nakano et al. (2013) from Landsat imagery. GLIMS (www.glims.org) and Randolph Glacier
135 Inventory (Arendt et al., 2012) quote over 1300 glaciers with a combined area of 1354 km². The
136 difference is due to the omission of the smaller glaciers in the eastern sector of the Caucasus in
137 this recent assessment.

138 The Greater Caucasus is subdivided into western, central and eastern sectors which have
139 average elevations of 3200 m, 4100 m, and 3700 m respectively. The most elevated central
140 sector extends between Mt. Elbrus (5642 m a.s.l.; Fig. 1) located several km north of the MCR
141 and Mt. Kazbek (5033 m a.s.l.; 42.7°N; 44.52°E). A characteristic feature of the Greater
142 Caucasus is a strong west-east precipitation gradient. The southern slope of the western MCR
143 receives over 2000 mm of precipitation while in the east, the annual total is about ten times lower
144 (Volodicheva, 2002). In response to the west-east precipitation gradients, the equilibrium line
145 altitude (ELA) changes rising from 2500-2700 m in the west through about 3200-3400 m in the
146 central sector to 3700-3950 m in the east. Due to greater precipitation in the south, ELA is lower
147 on the southern slopes especially in the central MCR and on Mt. Elbrus, where differences
148 between the southern and northern slopes reach 1000 m and 200-300 m respectively (Rototaeva
149 et al., 2006).

150 The largest glaciers are located in the central Greater Caucasus including the glaciated massif
151 of Mt. Elbrus. A number of larger valley glaciers have individual areas of 3-36 km². Cirque
152 glaciers with individual areas of 1 km² or less account for approximately 40% of the total. In the
153 western and eastern sectors, cirque glaciers with individual areas less than 3 km² prevail
154 (Rototaeva et al., 2006).

155

156 **3 Data and methods**

157 Changes in glacierized area and recession rates of glacier termini were assessed for the central
158 and western sectors of the MCR and Mt. Elbrus (Table 1; Fig. 1). Areas of 498 glaciers were
159 mapped of which 174 and 304 were located in the central and western sectors of the MCR

160 respectively on both northern (Russia) and southern (Georgia) slopes and twenty on Mt. Elbrus
161 (Table 1). The size of the smallest glacier mapped was 0.02 km².

162 Glacier outlines were mapped manually despite the advantages of automated mapping
163 demonstrated by Paul et al. (2009; 2013) because of the failure of the SWIR channel used in
164 automated classifications (Paul et al., 2002; Bolch et al., 2010) on ASTER in April 2008.
165 Extensive manual corrections are required when automatically mapping small glaciers (i.e. less
166 than 1 km², which constitute about 85% of all glaciers in the Caucasus) reducing the advantages
167 of automated techniques.

168

169 **3.1 Satellite imagery and glacier area mapping**

170 Two ASTER scenes from 2001 and 2010 were used for glacier mapping in the central MCR
171 (Table 1). ASTER imagery from 2010 was used for mapping glaciers in the western MCR,
172 however, earlier cloud-free imagery was not available and a Landsat ETM+ panchromatic image
173 from 2000, which has the same resolution of 15 m as ASTER, was used instead. For Mt. Elbrus,
174 ASTER scene was used for 2012 and panchromatic Landsat ETM+ was used for 1999 because
175 these are the only higher-resolution cloud-free images which cover the whole of Mt. Elbrus. An
176 ASTER 2001 scene, used for mapping in the central MCR, covers only the south-eastern sector
177 of Mt. Elbrus. To aid glacier mapping, a vast database of ground-based and aerial oblique
178 photographs was used (e.g. Fig. 2, 3).

179 The ASTER images were supplied by NASA Land Processes Distributed Active Archive
180 Center (LP DAAC) and Landsat ETM+ panchromatic images were downloaded from the US
181 Geological Survey (USGS; <http://glovis.usgs.gov/>). Both were supplied in the Universal
182 Transverse Mercator (UTM) zones 36-38 WGS 84 projection. The ASTER images were

183 orthorectified prior to the distribution (Lang and Welch, 1999). All satellite images were
184 acquired under [nearly] cloud-free conditions at the end of the ablation season (Table 1) when
185 glacier tongues were free of seasonal snow. On ASTER images, glacier outlines were mapped
186 using the 0.52-0.6 μm , 0.63-0.69 μm , and 0.78-0.86 μm bands. To aid the interpretation of the
187 panchromatic Landsat ETM+ image sharpening was applied using 5-4-3 band combination.
188 Where glacier margins were obscured by shadows from rocks and glacier cirque walls, a
189 contrast-stretching function was applied to the imagery using ENVI 4.6 software.

190 Most glaciers, except those located on Mt. Elbrus, have clearly defined ice divides. To avoid
191 errors associated with delineation of the upper boundaries of glaciers located on Mt. Elbrus, the
192 total glacierized area of the Elbrus massif was mapped and reported as the main outcome of this
193 study. To assess changes in individual glaciers, the ASTER GDEM and the hydrological tools
194 for basin delineation available in ARC 10.1 GIS and applied previously by Paul and Andreassen
195 (2009), Keinholz et al. (2013) and Svoboda and Paul (2009) were used for glacier delineation. It
196 was assumed that upper boundaries of glaciers on Mt. Elbrus did not change between 1999 and
197 2012.

198 Within the study area seven glaciers have been identified as surging by Rototaeva (2006).
199 These glaciers, were excluded from the analysis with the exception of the Kyukyurtlyu glacier
200 located on Mt. Elbrus. Although this glacier can exhibit changes that are not forced by climatic
201 variations, there was no evidence of surging within the assessment period.

202

203 **3.2 Quantification of errors**

204 For each glacier located in the MCR, we calculated three error terms resulting from (i) co-
205 registration of images, (ii) identification of glacier margins, and (iii) presence of debris cover on
206 glacier snouts.

207 The ASTER images, used for mapping glaciers in the central sector of the MCR, and ASTER
208 and panchromatic Landsat ETM+ images, used for mapping in the western sector of the MCR
209 and Mt. Elbrus, were co-registered using a network of 12 ground control points (GCP) for each
210 pair of images. Although ASTER imagery was used for both 2001 and 2010, co-registration of
211 these images and calculation of the resulting error term were required because different DEMs
212 were used in 2001 and 2010 (Meyer et al., 2011). The maximum root-mean-square error
213 ($RMSE_{x,y}$) was 8.1 m, which is less than the size of an ASTER pixel. The error of co-registration
214 was calculated following Granshaw and Fountain (2006). A buffer, with a width of half of the
215 $RMSE_{x,y}$ was created along the glacier outlines and the error term was calculated as an average
216 ratio of the original glacier areas to the areas with a buffer increment, resulting in an average
217 error of $\pm 1.2\%$. The errors of co-registration of ASTER and panchromatic Landsat ETM+
218 images used for mapping glaciers in the western MCR and on Mt. Elbrus were calculated using a
219 similar method. In the western Caucasus, $RMSE_{x,y}$ of 8.3 m and the error of $\pm 1.4\%$ were
220 achieved while on Mt. Elbrus, where the glacierized area is an order of magnitude larger than the
221 size of individual glaciers in the MCR, the error was $\pm 0.7\%$.

222 The uncertainty of glacier margin identification was estimated using multiple digitization
223 following Paul et al. (2013). A sub-sample of twenty glaciers from the MCR with areas of 0.5 -
224 9.8 km^2 was re-digitised ten times by three different operators. The average error was calculated
225 as 1.3% and used for the central and western MCR sub-samples. The error for the Elbrus
226 glacierized massif as a whole was very small at 0.2% due to (i) its large size and (ii) detailed

227 knowledge of the region obtained during many seasons of field work, including DGPS surveys
228 conducted since 2008 on individual glaciers (unpublished field records) and recent helicopter
229 surveys (e.g. Fig. 2).

230 Debris cover on glacier snouts is a major source of error in glacier mapping (Bhambri et al.,
231 2011; Bolch et al., 2008; Racoviteanu et al., 2008; Frey et al. 2012; Paul et al., 2013). In the
232 Caucasus, supra-glacial debris cover has lesser extent than in many glacierized regions,
233 especially in Asia (Stokes et al., 2007). Importantly, debris cover is not continuous on the snouts
234 of many glaciers in the MCR and most glaciers of Mt. Elbrus (Fig. 2). Most debris-covered
235 snouts do not merge with periglacial landforms thus making identification of glacier margins on
236 the satellite imagery easier.

237 To account for the error term due to debris cover, we followed Frey et al. (2012) and
238 increased the buffer size to two pixels (30 m) for the debris-covered segments of those glaciers
239 where supra-glacial debris was extensive. One of the most heavily debris-covered glaciers in the
240 Caucasus is Donguz-Orun (glacier tongue coordinates 43.231°N; 42.512°E) where supra-glacial
241 debris cover approximately 70% of the glacier as a result of avalanche nourishment supplying
242 debris from the headwall exceeding 4400 m a.s.l. (Fig. 3). For this specific glacier, the error of
243 mapping due to debris cover was calculated as $\pm 4.7\%$. We stress that (i) this glacier is not typical
244 of the region and (ii) this is the largest error in the whole data set. The debris cover term was
245 calculated for 67 glaciers and for most glaciers, it was below $\pm 1\%$.

246 The total error of glacier area change was calculated as a root mean square of the co-
247 registration, margin identification and, where applicable, debris-cover-related error terms.

248

249 **3.3 Assessment of changes in positions of glacier termini using aerial photographs**

250 Positions of the termini of 21 and 17 valley glaciers located in the central and western sectors of
251 the MCR respectively and of 6 glaciers located on the south-eastern slope of Mt. Elbrus were
252 measured on the satellite images and on the aerial photographs from 1987 (Table 1). The number
253 of measured valley glaciers (44 out of 97 in the sample) was restricted by the availability of
254 suitable aerial photographs. Glacier length and slope are the main controls of glacier snout
255 reaction (Hoelzle et al., 2003). All glaciers in the sample had similar slopes; the average lengths
256 (measured along the central flow line) of glaciers and length ranges are shown in Table 5.

257 Twenty six and seventeen aerial photographs with a resolution of 1-3 m were obtained on 25-
258 26 September 1987 under the nearly cloud-free conditions for central (including Mt. Elbrus) and
259 western sectors of the Greater Caucasus respectively (Table 1). The photographs were digitized
260 at 600 dpi resolution and co-registered to the 2001 ASTER and the 2000 Landsat ETM+
261 panchromatic images using 10-12 GCP per photograph. After co-registration, RMSE_{x,y} values
262 not exceeding 6.5 m were achieved for both ASTER and Landsat. ASTER 2001 and 2010
263 images were used to map retreat of glacier termini on Mt. Elbrus to make the retreat rates
264 comparable with the rest of the data set.

265 A change in glacier terminus position can be understood as a length measurement along a
266 central flow line (e.g. Stokes et al., 2006). However, changes in position of glacier termini are
267 not uniform along their margin. To account for this, five measurements were taken across the
268 width of each glacier terminus along flow lines and an average value was calculated in line with
269 similar studies (e.g. Koblet et al., 2010; Bhambri et al., 2012). The uncertainty in terminus
270 recession was calculated as a combination of the maximum RMSE_{x,y} of image co-registration
271 (8.1 m and 6.5 m for 2001-2010 and 1987-2001 periods in the central sector and 8.3 m and 6.5 m
272 in the western sector) and a half of pixel size of the satellite images (7.5 m) resulting in total

273 errors of ± 11.0 m and ± 9.9 m for the two assessment periods for the central sector and ± 11.2 and
274 ± 9.9 m for the western sector.

275

276 **3.4 Meteorological data**

277 There are two high-altitude meteorological stations with continuing observations in the study
278 area, Terskol in the central MCR (43.26°N ; 42.51°E ; 2141 m a.s.l.) and Klukhorskyi Pereval
279 (Path) in the western sector ($43^{\circ}15'8''\text{N}$; $41^{\circ}49'39''\text{E}$; 2037 m a.s.l.). Continuous records from
280 these stations are available from 1951 and 1960, respectively. Their monthly air temperature and
281 precipitation records were used to characterise climatic variations in the Baksan, Malka and
282 Kuban catchments on the northern slope. Continuous observations from the high-altitude regions
283 of the Inguri and Kodori catchments are not available. Records from Abastumani station, located
284 south of the study region (41.77°N ; 42.83°E ; 1265 m a.s.l.), available for the 1951-2005 period,
285 were used to characterise changes on the southern slope of the central MCR.

286

287 **4 Results**

288 **4.1 The Main Caucasus Ridge**

289 **4.1.1. Area change**

290 In total, 478 glaciers located in the central and western MCR lost 13.4 km^2 or $4.6 \pm 1.8\%$ of their
291 map area between 2000/2001 and 2010 (Table 2). Glaciers in the central MCR lost 8.6 km^2 or
292 $5.0 \pm 1.8\%$ of their area ($0.6\% \text{ a}^{-1}$); in the western sector, the area declined by 4.9 km^2 or
293 $4.1 \pm 1.9\%$ ($0.4\% \text{ a}^{-1}$). Overall, the differences between the slopes and sectors were small and
294 within uncertainty of the measurements. The greatest loss was observed on the southern slope in
295 the central MCR where glaciers lost $5.6 \pm 2.1\%$ of their combined map area in 9 years and the

296 lowest on the southern slope of the western MCR where glaciers lost $3.8\pm1.9\%$ although we note
297 that these differences are just within the uncertainty margin. Of all glaciers in the sample, twenty
298 lost over 20% of their 2000/2001 areas and forty one glaciers lost between 10% and 20%.

299 There are two compound-basin valley glaciers in the sample, both located in the Inguri
300 catchment. They experienced a slower recession than glaciers of other types (Table 3), losing
301 $2.80\pm1.8\%$ of their areas. Both glaciers are among the largest in the sample with 2001 areas of
302 31.4 km^2 (Lekzyri; the third largest glacier in the Caucasus and the largest in the sample) and 9.4 km^2
303 (Chalaati). There are no statistically significant differences in area loss between other types
304 of glaciers for the MCR as a whole, however, some differences between the northern and
305 southern slopes and the sectors were just outside the uncertainty margin (Table 3). Thus the
306 relative area loss by valley glaciers in the central sector of the MCR was twice as high as in the
307 western sector and valley glaciers located on the southern slope of the central MCR lost the
308 highest proportion of their map area in the whole sample. The valley glaciers in the central MCR
309 are larger than in the west and while their higher absolute loss (4.6 km^2 against 1.9 km^2 in the
310 west) is expected, a higher relative loss is not in line with trends observed in other regions and is
311 likely to result from lower precipitation in the central MCR in comparison with the west (see Fig.
312 6).

313 In contrast to other glacierized regions (e.g. Paul et al., 2004; Citterio et al., 2007) and in rare
314 agreement with DeBeer and Sharp (2007), the smallest glaciers exhibited the lowest relative
315 change in the central MCR. Thus glaciers with 2001 map areas of $0.02\text{-}0.1\text{ km}^2$ lost in total
316 $0.9\pm2.3\%$ of their combined area; this loss resulted from a 33% reduction in area of a single
317 glacier while another 36 did not exhibit measurable change. Glaciers within the $0.1\text{-}1.0\text{ km}^2$ and
318 $1.0\text{-}5.0\text{ km}^2$ categories lost $5.2\pm1.3\%$. Those larger than 5 km^2 lost 3.7%. In the western MCR,

319 the difference was less marked and within the uncertainty margin. Glaciers with 2000 map area
320 of 0.02-0.1 km² lost in total 3.9% of their combined area which is higher than in the central
321 sector despite higher precipitation. Glaciers with 2000/2001 map areas of 0.1-1.0 km² and 1.0 -
322 3.0 km² lost 4.7% and 3.2% respectively.

323

324 **4.2 Mt. Elbrus**

325 Glaciers located on Mt. Elbrus lost 5.8 km² or 4.9±0.7% (0.4 % a⁻¹) of their combined area
326 between 1999 and 2012. Their recession rate is comparable with glacier area loss in the MCR
327 despite the higher elevation and larger accumulation to ablation area ratios (AAR) of the Elbrus
328 glaciers (Table 4; Fig. 4). A characteristic feature of glacier recession on Mt. Elbrus is the
329 expansion of nunataks, exposed rocks and separation of sections of glaciers in the ablation zone
330 below approximately 4000 m a.s.l. Nunataks and exposed rocks were not accounted for in the
331 previous measurements (e.g. Zolotarev and Kharkovets 2012) although their combined area was
332 4.14 km² or 3.5% of the Elbrus glaciated massif in 1999. In 2012, their combined area was 3.74
333 km². However, the reduction in their absolute area is misleading because in the lower parts of the
334 ablation zone they merged with the surrounding rocks. Calculated relatively to the boundaries of
335 glaciated area as in 1999, the area of 'nunataks' and exposed rocks was approximately 6 km².
336 Fig. 5 illustrates the expansion of exposed rocks on the southern slope of Mt. Elbrus including
337 Bolshoi Azau, Malyi Azau and Garabashi glaciers. Two areas of exposed rocks expanded
338 considerably over the last decade, e.g. between Bolshoi Azau and Malyi Azau glaciers (Fig. 5 b).
339 In all, eight small ice bodies with a total area of 0.3 km² had separated from the main glacier
340 massif by 2012.

341 Changes in areas of individual glaciers are summarized in Table 4. In absolute terms, the
342 Bolshoi Azau and Dzhikiugankez glaciers experienced the largest recession losing 1.2 km² and
343 1.9 km². In relative terms, two small hanging glaciers (N 311 and 312) located west of the
344 Bolshoi Azau glacier (Fig. 4 and 5) lost the largest proportion of their map area, 15.2% and
345 15.4% each, although in absolute terms the loss is small at 0.1 km². The larger glaciers lost
346 between 1% and 7.4%. Among the larger glaciers, the highest relative loss characterised
347 Dzhikiugankez ice plateau, Garabashi and Irikchat glaciers. The area losses of Glacier N 317
348 (Fig. 4), which terminates over a cliff at approximately 4400 m a.s.l., and Glacier N 319 were not
349 detectable. The difference in area loss between glaciers with different aspect is close to the
350 accuracy of measurements for glaciers with southern (5.6%), eastern (5.0%) and northern (4.3%)
351 aspect. The three glaciers with western aspect lost 2.5% of their areas.

352

353 **4.3 Teminus retreat**

354 Data on retreat of glacier termini are summarised in Table 5. Across the region, terminus retreat
355 increased from the 1987-2000/2001 period to the 2000/2001-2010 period by the factor 2.5 – 3.8.
356 The highest recession rates of 11-14 m a⁻¹ were observed in the central MCR and on Mt. Elbrus,
357 where glaciers are larger, with the strongest acceleration on the southern slope of the MCR. The
358 largest total retreat was exhibited by the Bolshoi Azau glacier, located on Mt. Elbrus, which is
359 the second largest glacier in the sample. This glacier lost 500 m, retreating at a steady rate of 22
360 m a⁻¹. The largest glacier in the sample, Lekzyri, located on the southern slope, lost 40 m and 200
361 m (2.5% of its 2001 length) in the two periods respectively. Two benchmark glaciers, Djankuat
362 and Garabashi, retreated by 185 m and 170 m in total. Retreat of glacier termini in the western

363 sector was more subdued, especially on the southern slope, where glaciers were receding by 3.2
364 m a⁻¹ in the first decade of the 21st Century.

365

366 **4.4 Climatic variability**

367 The observed glacier recession is consistent with increasing air temperature of the ablation
368 season (June-July-August; JJA) registered in both central and western MCR (Fig. 6 a). In the
369 central MCR, at Terskol station, the average JJA temperatures in 1987-2001 and 2001-2010 were
370 11.6°C and 11.7°C respectively, exceeding the mean JJA temperature of 10.9°C registered
371 between 1960 and 1986. Similar trends are observed in the western MCR where the average JJA
372 temperatures at Klukhorskyi Pereval station in 1987-2001 and 2001-2010 were 12.3°C and
373 12.5°C respectively exceeding the 1960-1986 mean JJA temperature of 11.8°C. The JJA
374 temperature record from Abastumani (not shown) is intermittent and terminates in 2005,
375 however, it correlates closely with the Terskol record ($r=0.90$) in the overlapping period and
376 indicates strong climatic warming between the 1980s and 2005. It should be noted, however, that
377 despite the warming observed in the last two decades, the 1951-1960 decade still remains the
378 warmest on record in the central MCR with an average JJA temperature of 12.4°C (Fig. 6a).

379 An increase in the accumulation season (October-April) precipitation, statistically significant
380 at 95% confidence level, was registered at both Terskol and Klukhorskyi Pereval in the 1987-
381 2010 period, when the averages of 538 mm and 1173 mm exceeded the 1960-1986 averages of
382 427 mm and 1037 mm by 26% and 13% respectively (Fig. 6b). At Terskol, a positive linear trend
383 for the 1951-2011 period was statistically significant. It indicated a 35 mm increase in the
384 accumulation season precipitation per decade and explained 19% of the total variance in the data
385 set. By contrast, the accumulation season precipitation did not change at Abastumani in 1987-

386 2005 in comparison with 1960-1986. By 2005, a statistically significant change in precipitation
387 had already occurred on the northern slope at both stations.

388

389 **5 Discussion**

390 In the central and western sectors of the MCR and on Mt. Elbrus, the measured glacier map area
391 reduction in the first decade of the 21st Century of $4.7 \pm 1.6\%$ exceeded uncertainties associated
392 with image co-registration, delineation of glacier outlines and presence of debris cover (Table 2).
393 The total mapping error for ASTER imagery was estimated as $\pm 1.8\%$ and $\pm 1.9\%$ for the central
394 and western MCR glaciers respectively and $\pm 0.7\%$ for Mt. Elbrus. This is considerably lower
395 than errors resulting from the use of Landsat imagery (e.g. Stokes et al., 2006; Bhambri et al.,
396 2011) and slightly lower than in other studies utilising ASTER imagery (e.g. Paul et al., 2004;
397 Bhambri et al., 2011; Shahgedanova et al., 2012). The latter difference is due to the limited
398 extent of debris cover, size distribution and morphology of glaciers in the sample. The supra-
399 glacial debris cover significantly reduces the accuracy of glacier mapping (e.g. Racoviteanu et
400 al., 2008; Bhambri et al., 2011). However, in the Caucasus the extent of supra-glacial debris is
401 relatively small, typically accounting for 3-25% of individual glacier areas (Stokes et al., 2007)
402 with a few exceptions such as Donguz-Orun. Importantly, debris-covered glaciers have clearly
403 identifiable snout margins. Larger errors arise when mapping very small glaciers with map areas
404 below 0.1 km² (e.g. Shahgedanova et al., 2012), however, only 20% of the glaciers in the
405 assessed sample were smaller than 0.1 km² in 2001 and these were mostly cirque glaciers with
406 clearly defined margins.

407 Although differences between glacier wastage in different sectors of the MCR are close to the
408 measurement uncertainty, it is possible to suggest that glaciers located on the southern slope of

409 the central MCR lost a higher proportion of their area than glaciers in other regions of the
410 Caucasus, $5.6 \pm 2.1\%$ (Table 2). The valley glaciers lost even higher proportion, 7.4% (Table 3)
411 which is the highest value in the whole sample. A higher rate of glacier wastage in the south is
412 consistent with the observed trends in precipitation. Negative precipitation anomalies were
413 observed in on the southern slope in the 1990s. In the 2000s, precipitation anomalies were
414 positive but lower than in the north (Fig. 6b). These trends are consistent with the impacts of
415 NAO on precipitation in southern Europe and westernmost regions of Asia (Marshall et al.,
416 2001). By contrast, glaciers on the southern slope of the western MCR lost 3.8% of their area
417 which is the lowest wastage in the region (Table 2) with valley glaciers losing 2.9% in the north
418 and 3.6% in the south (Table 3). It is likely that high accumulation season precipitation,
419 exceeding that in the central MCR by the factor of 2-3 (Volodicheva, 2002) and persistent
420 positive precipitation anomalies observed since the mid-1990s, slowed down glacier retreat in
421 the western MCR.

422 The glaciers on Mt. Elbrus lost the same percentage of their combined area as glaciers in the
423 central MCR despite the higher AAR (Table 2). We calculated the area reduction as $4.9 \pm 0.7\%$
424 with a rate of decrease of $0.4\% \text{ a}^{-1}$ between 1999 and 2012. Zolotarev and Kharkovets (2012),
425 who assessed glacier area change on Mt. Elbrus in the 1997-2007 period using aerial
426 photography from 1997 and Cartosat-1 imagery with spatial resolution of 2.5 m, reported an
427 overall 3.8% area loss. The difference between the two assessments is small and, in addition to
428 measurement uncertainties, reflects slightly different periods of assessments and interpretation of
429 nunataks and bare rocks as glacierised area by Zolotarev and Kharkovets (2012). Holobaca
430 (2013) reported area change of 9.1% between 1985 and 2007 ($0.4\% \text{ a}^{-1}$) from Landsat TM
431 imagery which is the same as in our assessment.

432 The average rate of terminus recession of valley glaciers doubled in the north and more than
433 tripled in the south in the 21st Century in comparison with 1987-2001. Using the approximation
434 by Johannesson et al. (1989) based on a ratio between glacier depth at ELA and mass balance near
435 the glacier terminus, dynamic response times of Djankuat and Garabashi glaciers are estimated
436 as 12-15 and 17-18 years respectively. The observed glacier recession and its acceleration in the
437 last decade detected from the changes in the rate of snout retreat are consistent with the positive
438 trend in summer air temperatures since the 1990s. Strong positive anomalies of 2°C in 2006 and
439 2010 (Fig. 6a) contributed to enhanced glacier melt (Fig. 7). The exceptional heat wave which
440 developed over European Russia in July-August 2010 (Grumm, 2011) was as detrimental for the
441 state of the Caucasus glaciers as the 2003 West European heat wave for the glaciers in the Alps
442 (Haeberli et al., 2007). The mass balance records for Garabashi show that in the summer of 2010
443 alone, the glacier lost 2.52 m w.e., close to the record loss of 2.58 m w.e. in the El Niño year of
444 1998 and nearly twice the long-term average (1984 to current). A strong decline in cumulative
445 mass balance (Fig. 7) occurred after 1998 despite a 20% increase in precipitation (Fig. 6b) north
446 of MCR (WGMS, 2013).

447 Glacier shrinkage in the Caucasus appears to be slower than in the European Alps. Paul et al.
448 (2004) reported 18% ($1.3\% \text{ a}^{-1}$) glacier shrinkage in the Swiss Alps in the 1985-1999 period.
449 Maragno et al. (2009) reported 5.5% ($1.4\% \text{ a}^{-1}$) shrinkage in 1999-2003 and even stronger
450 shrinkage of 11% or $2.8\% \text{ a}^{-1}$ was reported by Diolaiuti et al. (2011) for the Italian Alps. The
451 heat wave of 2003 had a strong impact on glacier wastage in the European Alps (Haeberli et al.,
452 2007), however, even prior to this extreme event, glacier wastage rates in the Alps exceeded
453 those of $0.4\text{--}0.6\% \text{ a}^{-1}$ that we report for the Caucasus. Another important difference is
454 contribution of small glaciers to the overall reduction of glacierized area. Thus in the Swiss and

455 Lombardy Alps, glaciers with individual areas less than 1 km² contributed about 40% and 58%
456 of total area loss while accounting for only 15% and 30% of glacierized area respectively (Paul
457 et al., 2004; Citterio et al., 2007). Glaciers of the same size category occupied 22.3% of the
458 glacierized area in MCR and contributed 7.3% of area loss.

459

460 **6 Summary**

461 To summarise, (i) the Caucasus glaciers lost 4.7±1.6% of their total area between 2000 and
462 2010/2012 and this estimate exceeds the uncertainty of the measurements; (ii) glaciers of Mt.
463 Elbrus lost a similar proportion of their area despite higher elevation and large AAR; (iii) the
464 largest wastage occurred on the southern slope of the central sector in line with precipitation
465 anomalies; (iv) the retreat of glacier termini accelerated in the first decade of the 21st century in
466 comparison with the end of the 20th century.

467

468 **References**

469 Andreassen, L.M., Paul, F., Kääb, A. and Hausberg, J.E.: Landsat-derived glacier inventory for
470 Jotunheimen, Norway, and deduced glacier changes since the 1930s. *The Cryosphere*, 2, 131-
471 145, doi:10.5194/tc-2-131-2008, 2008.

472 Arendt, A. et al. (79 authors): Randolph Glacier Inventory [v2.0]: A Dataset of Global Glacier
473 Outlines, Boulder, Colorado, Digital Media, <http://www.glims.org/RGI/randolph.html> (last
474 access: 7 July 2014), 2012.

475 Bhambri, R., Bolch, T., Chaujar, R.K. and Kulshreshtha S.C.: Glacier changes in the Garhwal
476 Himalaya, India, from 1968 to 2006 based on remote sensing. *J. Glaciol.*, 57 (203), 543-556,
477 2011.

478 Bhambri, R., Bolch, T., and Chaujar, R.K.: Frontal recession of Gangotri Glacier, Garhwal
479 Himalayas, from 1965-2006, measured through high resolution remote sensing data. Current
480 Science, 102, 489-494, 2012.

481 Bolch, T., Buchroithner, M.F., Pieczonka, T., Kunert, A.: Planimetric and volumetric glacier
482 changes in the Khumbu Himalaya 1962 – 2005 using Corona and ASTER data. J. Glaciol.,
483 54(187), 562-600, 2008.

484 Bolch, T., Menounos, B. and Wheate, R.: Landsat-based inventory of glaciers in western
485 Canada, 1985–2005, Rem. Sens. Environ., 114, 127–137, 2010.

486 Borovik, E.S. and Kravtsova, V.I.: Catalogue of Glaciers of the USSR, Gidrometeoizdat,
487 Leningrad, Vol. 8, Part 5, Basins of the Malka and the Baksan Rivers, 86 pp., 1970 (in
488 Russian).

489 Bushueva, I.S. and Solomina, O.N.: Kolebaniya lednika Kashkatash v XVII-XXI vv. po
490 kartograficheskim, dendrochronologicheskim i lichonometricheskim dannym (Fluctuations of
491 Kashakatash Glacier in XVII-XXI centuries according to cartographic, dendrochronological
492 and lichonometric data). Led i Sneg (Ice and Snow), 2 (118), 121-130, 2012 (in Russian).

493 Church, J.A., White, N.J., Konikow, L.K., Domingues, C. M. ., Cogley, J. G., Rignot, E.,
494 Gregory, J. M., van den Broeke, M. R., Monaghan, A. J. and Velicogna, I.: Revisiting the
495 Earths sea-level and energy budgets from 1961 to 2008, Geophys. Res. Lett., L18601,
496 doi:10.1029/2011GL048794, 2012.

497 Citterio, M., Diolaiuti, G., Smiraglia, C., D'Agata, C., Carnielli, T., Stella, G. and Siletto, G.B.:
498 The fluctuations of Italian glaciers during the last century: A contribution to knowledge about
499 Alpine glacier changes. Geogr. Annal. A, 89 A, 167-184, 2007.

500 DeBeer, C.M. and Sharp, M.J.: Recent changes in glacier area and volume within the Southern
501 Canadian Cordillera, *Ann. Glaciol.*, 46 (1), 215–221, 2007.

502 Diolaiuti, D., Maragno, D., D'Agata, C., Smiraglia,C., and Bocchiola, D.: Glacier retreat and
503 climate change: Documenting the last 50 years of Alpine glacier history from area and
504 geometry changes of Dosde Piazzi glaciers (Lombardy Alps, Italy). *Prog. Phys. Geog.*, 35,
505 161-182, 2011.

506 Dolgova, E.A., Matskovsky, V.V., Solomina, O.N., Rototaeva, O.V., Nosenko, G.A., and
507 Khmelevsky, I.F.: Reconstructing mass balance of Garabashi Glacier (1800-2005) using
508 dendrochronological data, *Led i Sneg* (Ice and Snow), 1 (121), 34-43, 2013 (in Russian).

509 Dyurgerov, M.B. and Meier, M.F: Twentieth century climate change: evidence from small
510 glaciers. *P. Nat. Acad. Sci. USA*, 97, 1406-1411, 2000.

511 Frey, H., Paul, F. and Strozzi, T.: Compilation of a glacier inventory for the western Himalayas
512 from satellite data: methods, challenges, and results. *Rem. Sens. Environ.*, 124: 832-843, 2012.

513 Granshaw, F.D. and Fountain, A.G.: Glacier change (1958-1998) in the North Cascades National
514 Park Complex, Washington, USA. *J. Glaciol.*, 52 (177), 251-256, 2006.

515 Grumm, R.H.: The Central European and Russian heat event of July-August 2010. *B. Am.
516 Meteorol. Soc.*, 92: 1285-1296, 2011.

517 Haeberli, W., Hoelzle, M., Paul, F. and Zemp, M.: Integrated monitoring of mountain glaciers as
518 key indicators of global climate change: the European Alps. *Ann. Glaciol.*, 46 (1), 150-160,
519 2007.

520 Hoelzle, M., Haeberli, W., Dischl, M. and Peschke, W.: Secular glacier mass balances derived
521 from cumulative glacier length changes. *Glob. Plan. Change*, 36, 295-306, 2003.

522 Holobaca, I-H: Glacier Mapper – a new method designed to assess change in mountain glaciers,
523 Int. J. Rem. Sens., 34 (23), 8475-8490, 2013.

524 IPCC 2013: Climate Change 2013: The Physical Science Basis. Contribution of Working Group
525 I to the Fifth Assessment Report of the Intergovernmental Panel on Climate Change, edited by:
526 Stoker, T.F., Qin, D., Plattner, G-K., Tignor, M., Allen, S.K., Boschung, J., Nauels, A., Xia,
527 Y., Bex, V., and Midgley, P.M. Cambridge University Press, Cambridge, 1535 pp.

528 Jóhannesson, T., Raymond, C. and Waddington, E.: Time-scale for adjustment of glaciers to
529 changes in mass balance. J. Glaciol., 35 (121), 355– 369, 1989.

530 Keinholz, C., R. Hock, and A.A. Arendt: A new semi-automatic approach for dividing glacier
531 complexes into individual glaciers. J. Glaciol., 59 (217), 925-937, 2013.

532 Koblet, T., Gartner-Roer, I., Zemp, M., Jansson, P., Thee, P., Haeberli, W. and Holmlund, P.:
533 Reanalysis of multi-temporal aerial images of Storglaciaren, Sweden (1959–99) – Part 1:
534 Determination of length, area, and volume changes. The Cryosphere, 4, 333-343,
535 doi:10.5194/tc-15 4-333-2010,2010.

536 Kutuzov S., Lavrentiev, I.I., Macheret, Yu. Ya. and Petrakov, D.A.: Changes of Marukh Glacier
537 from 1945 to 2011 Led i Sneg (Ice and Snow), 1 (117), 123-128, 2012 (in Russian).

538 Lang, H.R., and Welch, R.: ATBD-AST-08 Algorithm theoretical basis document for ASTER
539 digital elevation models (Standard product AST14),
540 http://eospso.gsfc.nasa.gov/eos_homepage/for_scientists/atbd/docs/ASTER/atbd-ast-14.pdf,
541 (last access: 7 July 2014), 1999.

542 Leclercq, P.W. and Oerlemans, J.: Global and hemispheric temperature reconstruction from
543 glacier length fluctuations. Clim. Dyn., 38: 1065-79, 2012.

544 Leclercq, P.W., Oerlemans, J., Basagic, H. J., Bushueva, I., Cook, A. J., and Le Bris, R.: A data
545 set of worldwide glacier length fluctuations, *The Cryosphere*, 8, 659-672, doi:10.5194/tc-8-
546 659-2014, 2014.

547 Maragno, D., Diolaiuti, G., D'Agata, C., Mihalcea, C., Bocchiola, D., Janetti, E.B., Riccardi, A.
548 and Smiraglia, C.: New evidence from Italy (Adamello Group, Lombardy) for analyzing the
549 ongoing decline of Alpine glaciers. *Geograf. Fis. Dinam. Quaternaria*, 32, 31-39, 2009.

550 Marshall, J., Kushnir, Y., Battisti, D., Chang, P., Czaja, A., Dickson, R., Hurrell, J., McCartney,
551 M., Saravanan, R., and Visbeck, M.: North Atlantic climate variability: phenomena, impacts
552 and mechanisms. *Int. J. Climatol.*, 21, 1863-1898, 2001.

553 Maruashvili, L.I., Kurdgelaidze, G.M. and Lashkhi, T.A.: Catalogue of Glaciers of the USSR,
554 Vol. 9, Parts 2-6, Basin of the Kodori and Inguri Rivers, Gidrometeoizdat, Leningrad, 86 pp.,
555 1975 (in Russian).

556 Meyer, D., Tachikawa, T., Kaku, M., Iwasaki, A., Gesch, D., Oimoen, M., Zhang, Z., Danielson,
557 J., Krieger, T., Curtis, B., Haase, J., Abrams, M., Crippen, R., and Carabajal, C.: ASTER
558 Global Digital Elevation Model Version 2 – Summary of Validation Results. NASA Land
559 Processes Distributed Active Archive Center, online report <http://www.jspacesystems.or.jp/>
560 ersdac/GDEM/ver2Validation/Summary_GDEM2_validation_report_final.pdf (last access: 7
561 July 2014), 26 pp., 2011.

562 Nakano, K., Zhang, Y., Shibuo, Y., Yabuki, H. and Hirabayashi, Y.: A monitoring system for
563 mountain glaciers and ice caps using 30 meter resolution satellite data. *Hydrol. Res. Let.*, 7(3),
564 73–78, 2013.

565 Panov, V.D.: *Evolyutsiya sovremennoego oledeneniya Kavkaza* (Evolution of the Contemporary
566 Glaciation in the Caucasus), Gidrometeoizdat. St. Petersburg, 432 pp, 1993 (in Russian).

567 Panov, V.D. and Kravtsova, V.I.: Catalogue of Glaciers of the USSR, Vol. 8, Parts 1-4, Basin of
568 the Kuban River, Gidrometeoizdat, Leningrad, 145 pp., 1967 (in Russian).

569 Paul, F., Kääb, A., Maisch, M., Kellenberger, T. and Haeberli, W.: The new remote-sensing-
570 derived Swiss glacier inventory: I. Methods. *Ann. Glaciol.*, 34, 355–361, 2002.

571 Paul, F., Kääb, A., Maisch, M., Kellenberger, T. and Haeberli, W.: Rapid disintegration of
572 Alpine glaciers observed with satellite data. *Geophys. Res. Lett.*, 31(21), L21402,
573 10.1029/2004GL020816, 2004.

574 Paul, F. and Andreassen, L.M.: A new glacier inventory for the Svartisen region, Norway, from
575 Landsat ETM+ data: challenges and change assessment. *J. Glaciol.*, 55 (192), 607-618, 2009.

576 Paul, F., Barry, R., Cogley, G., Frey, H., Haeberli, W., Ohmura, A., Omanneney, S., Raup, B.,
577 Rivera, A., and Zemp, M.: Recommendations for the compilation of glacier inventory data
578 from digital sources, *Ann. Glaciol.*, 50 (53), 119-126, 2009.

579 Paul, F., Barrand, N.E., Baumann, S., Berthier, E., Bolch, T., Casey, K., Frey, H., Joshi, S.P.,
580 Konovalov, V., Le Bris, R., Mölg, N., Nosenko, G., Nuth, C., Pope, A., Racoviteanu, A.,
581 Rastner, P., Raup, B., Scharrer, K., Steffen, S. and Winsvold, S: On the accuracy of glacier
582 outlines derived from remote-sensing data, *Ann. Glaciol.*, 54(63), 171-182, 2013.

583 Popovnin, V.V.: Pole akkumulyatsii gornogo lednika (Accumulation Zone of a Mountain
584 Glacier) Mater. Glyatsiol. Issled., (Data Glaciol. Res.), 88, 27– 40, 2000 (in Russian).

585 Popovnin, V.V. and Petrakov, D.A.: Lednik Djankuat za poslednie 34 goda, 1967/68-2000/01
586 (Djankuat Glacier in the last 34 years, 1967/68-2000/01). Mater. Glyatsiol. Issled., (Data
587 Glaciol. Res.), 98, 167-175, 2005 (in Russian).

588 Rototaeva, O. Data on surging glaciers in the Northern Caucasus, in: Oledenenie Severnoi i
589 Tsentralnoi Evrazii v Sovremennyyu Epohu (Glaciation in Northern and Central Eurasia at

590 Present Time), edited by: Kotlyakov, V.M., Nauka Publishers, Moscow, 215-223, 2006 (in
591 Russian).

592 Rototaeva, O., Nosenko, G., Tarasova, L., and Khmelevsky, I.: Caucasus, in Oledenenie
593 Severnoi i Tsentralnoi Evrazii v Sovremennyyu Epohu (Glaciation in Northern and Central
594 Eurasia at Present Time), edited by: Kotlyakov, V.M., Nauka Publishers, Moscow, 141-162,
595 2006 (in Russian).

596 Racoviteanu, A.E., Williams, M.W. and Barry, R.G.: Optical Remote Sensing of Glacier
597 Characteristics: A Review with Focus on the Himalaya. *Sensors*, 8, 3355-3383, 2008.

598 Shahgedanova, M., Stokes, C.R., Gurney, S.D. and Popovnin, V.V.: Interactions between mass
599 balance, atmospheric circulation and recent climate change on the Djankuat glacier, Caucasus
600 Mountains, Russia, *J. Geophys. Res.–Atm.*, 110 (D4), D04108, 10.1029/2004JD005213, 2005.

601 Shahgedanova, M., Popovnin, V., Aleynikov, A., Petrakov, D. and Stokes, C.R.: Long-term
602 change, inter-annual, and intra-seasonal variability in climate and glacier mass balance in the
603 central Greater Caucasus, Russia, *Ann. Glaciol.*, 46 (1), 355-361, 2007.

604 Shahgedanova, M., Nosenko, G., Bushueva, I. and Ivanov, M.: Changes in area and geodetic
605 mass balance of small glaciers, Polar Urals, Russia, 1950-2008. *J. Glaciol.*, 58 (211), 953-964,
606 2012.

607 Stokes, C.R., Gurney, S.D., Shahgedanova, M. and Popovnin, V.V.: Late-20th-century changes
608 in glacier extent in the Caucasus Mountains, Russia/Georgia, *J. Glaciol.*, 52 (176): 99-109,
609 2006.

610 Stokes, C.R., Popovnin, V.V., Aleynikov, A. and Shahgedanova, M.: Recent glacier retreat in the
611 Caucasus Mountains, Russia, and associated changes in supraglacial debris cover and
612 supra/proglacial lake development. *Ann. Glaciol.*, 46 (1), 196-203, 2007.

613 Svoboda, F. and Paul, F.: A new glacier inventory on southern Baffin Island, Canada, from ASTER data:
614 I. Applied methods, challenges and solutions, *Ann. Glaciol.*, 50 (53), 11-21, 2009.

615 Volodicheva, N.: The Caucasus, in *The Physical Geography of Northern Eurasia*, edited by:
616 Shahgedanova, M., 350– 376, Oxford University Press, Oxford, 2002.

617 WGMS: *Glacier Mass Balance Bulletin No. 12 (2010-2011)* and earlier issues edited by: Zemp,
618 M., Nussbaumer, S.U., Gärtnner-Roer, I.I., Hoelzle, M., Paul, F. and Haeberli, W., ICSU(WDS)
619 / IUGG (IACS) / UNEP / WMO. *World Glacier Monitoring Service*, Zurich, Switzerland, 106
620 pp., 2013.

621 Yefremov, Yu.V., Panov, V.D., Lurie, P.M., Iliychev, Yu.S., Panova, S.V., and Lutkov, D.A.:
622 Orografiya, oledenenie, klimat Bolshogo Kavkaza (Orography, Glaciation and Climate of the
623 Greater Caucasus). Kubanskyi State University Press, Krasnodar, 337 pp., 2007 (in Russian).

624 Zemp, M., Hoelzle, M. and Haerberli, W.: Six decades of glacier mass-balance observations: a
625 review of the worldwide monitoring network. *Ann. Glaciol.*, 50 (50), 101-111, 2009.

626 Zolotarev, E.A. and Kharkovets, E.G.: *Oledenenie Elbrusa kontse XX veka* (Glaciation of Mt.
627 Elbrus at the end of the 20th Century). *Led i Sneg* (Ice and Snow), 5 (112), 45-51, 2007 (in
628 Russian).

629 Zolotarev, E.A. and Kharkovets, E.G.: *Evolyutsiya oledeneniya Elbrusa posle malogo*
630 *lednikovogo perioda* (Evolution of glaciation on Mt Elbrus after the Little Ice Age). *Led i Sneg*
631 (Ice and Snow), 2 (118), 5-14, 2012 (in Russian).

632

633 Table 1 Details of the imagery used for glacier mapping. Location of catchments are shown
 634 in Fig. 1.

Date	Type of imagery	Region	No of glaciers
6/09/2012	ASTER	Mt. Elbrus 42.96-43.60°N; 42.16-43.05°E	20
18/08/1999	Landsat ETM+ panchromatic; path 171; row 030	Mt. Elbrus 41.14-44.19 °N; 41.94-44.96°E	
15/09/2001	ASTER	Central MCR and Mt. Elbrus for the assessment of recession of glacier termini; 43.05-43.35°N; 42.34-42.83°E	174 in all: 99, 9 and 69 on northern and southern slopes in Baksan, Malka and Inguri catchments respectively
23/08/2010	ASTER	Western MCR; 43.07-43.43°N; 41.62-42.40°E	304 in all: 147 and 157 on northern (Kuban catchment) and southern (Inguri and Kodori catchments) slopes
25-26/09/1987	Aerial photographs	43.05-43.35°N; 42.34-42.83°E	28 glaciers: 7 in the Baksan and Adylsu valleys and 14 in the Inguri valley in central MCR; 6 on south-eastern slope of Mt. Elbrus
25-26/09/1987	Aerial photographs	43.07-43.43°N 41.80-42.40°E	17 glaciers in the Kuban, Kodory and Inguri basins in the western MCR

635

636

637 Table 2. Changes in glacierized area.

Region		Combined area (km ²)		Area reduction	
		1999/2000/2001	2010/2012	km ²	%
Central MCR	Total	170.63	162.07	8.56	5.0±1.8
	Northern	73.41	70.28	3.13	4.3±1.6
	Southern	97.22	91.79	5.43	5.6±2.1
Western MCR	Total	118.3	113.4	4.87	4.1±1.9
	Northern	63.15	60.38	2.77	4.4±1.9
	Southern	55.15	53.05	2.1	3.8±1.9
Elbrus		118.4	112.6	5.8	4.9±0.7
Total		407.35	388.11	19.24	4.7±1.6

638

639 Table 3. Area loss (%) according to glacier type in the Central and Western MCR. Number of
640 glaciers of each type is given in parentheses. The two compound-valley glaciers located on the
641 southern slope of the central MCR are not included (see text).

Region	Central			Western			All
	North	South	All	North	South	All	
Type							
Valley	5.3 (7)	7.4 (25)	6.7	2.9 (19)	3.6 (42)	3.3	5.0
Cirque	4.1 (156)	3.3 (20)	4.0	6.2 (104)	4.4 (85)	5.5	4.6
Hanging	4.5 (4)	0 (3)	4.4	6.6 (23)	0.8 (6)	5.2	5.1
Ice aprons	5.9 (7)	6.8 (15)	6.1	3.5 (11)	4.0 (24)	3.7	5.0

642

643

644 Table 4. Changes in map areas of glaciers located on Mt. Elbrus between 1999 and 2012. All
 645 glaciers are shown in Fig.4.

Number (Fig. 4)	Glacier		Area		Area change	
	Name	WGI ID	1999	2012	km ²	%
1	Ulluchiran	SU4G08005001	11.63	11.13	0.5	4.3
2	Karachaul	SU4G08005002	7.44	7.22	0.22	3.0
3	Ullukol and Ullumalienderku	SU4G08005003	4.85	4.54	0.31	6.4
4	Mikelchiran	SU4G08005005	5.05	4.86	0.19	3.8
5	Dzhikiugankez	SU4G08005006	26.12	24.22	1.90	7.3
6	Irikchat	SU4G08005018	1.41	1.31	0.10	7.1
7	Irik	SU4G08005020	9.18	8.90	0.28	3.1
8	No 25	SU4G08005025	0.60	0.56	0.04	6.7
9	Terskol	SU4G08005026	7.99	7.71	0.28	3.5
10	Garabashi	SU4G08005027	3.26	3.02	0.24	7.4
11	Malyi Azau	SU4G08005028	8.84	8.27	0.57	6.4
12	Bolshoy Azau	SU4G08005029	19.70	18.53	1.17	5.9
13	311	SU4H08004311	0.46	0.39	0.07	15.2
14	312	SU4H08004312	0.26	0.22	0.04	15.4
15	313*	SU4H08004313	1.07	1.05	0.02	1.9
16	Ullukam*	SU4H08004313	0.65	0.64	0.01	1.5
17	317	SU4H08004317	0.55	0.55	0.00	0.00
18	Kyukyurtlyu	SU4H08004318	6.92	6.83	0.09	1.3
19	319	SU4H08004319	0.46	0.46	0.00	0.00

20	Bityuktyube	SU4H08004320	1.98	1.90	0.08	4.0
	8 separated ice bodies (Fig. 4)		-	0.3	-	-
Total			118.4	112.6	5.8**	4.9±0.7

646 * Glacier N 313 is a now disconnected part of Ullukam hence the same WGI identification

647 number.

648 ** Including 8 separated ice bodies in 2012

649

650 Table 5. Characteristics of glaciers used for measuring snout retreat. The average error terms are
 651 ± 9.9 m and ± 11 m for the 1987-2000/2001 and 2000/2001-2010 periods respectively.

Region	Slope	No	Length (km) as in 1987	Length change					
				1987-2000/2001		2000/2001-2010			
				Average	Range	m	$m a^{-1}$		
Central	All	21	4.2	0.8-9.7	52.9	3.8	106.7	11.9	
	MCR	N	7	4.6	2.8-9.7	77.1	5.5	121.4	13.5
		S	14	4.0	0.8-8.3	40.8	2.9	99.4	11.0
Western	All	17	2.3	0.8-3.6	40.5	3.2	78.5	8.7	
	MCR	N	13	2.2	0.8-3.6	47.5	3.7	88.6	8.9
		S	4	2.7	1.8-3.3	13.3	1.0	32.7	3.2
Elbrus	SE	6	7.0	2.6-10.2	115.8	8.3	126.7	14.1	

652

653

654 **Figure captions**

655 Figure 1. Study area and satellite imagery used for the analysis. The yellow lines show the Black
656 Sea coastline, the MCR, and the catchment boundaries. The catchments are numbered as
657 follows: (1) Kuban; (2) Malka; (3) Baksan; (4) Inguri; and (5) Kodori.

658 Figure 2. Oblique aerial photograph of (a) glaciers on Mt. Elbrus and (b) snout of the Malyi
659 Azau glacier. Note the clearly defined glacier boundaries and a very limited extent of debris
660 cover. Photograph by I.I. Lavrentiev (25 August 2009).

661 Figure 3. Oblique aerial photograph of the Donguz-Orun glacier which has the highest extent of
662 debris cover in the sample. Photograph by I.I. Lavrentiev (25 August 2009).

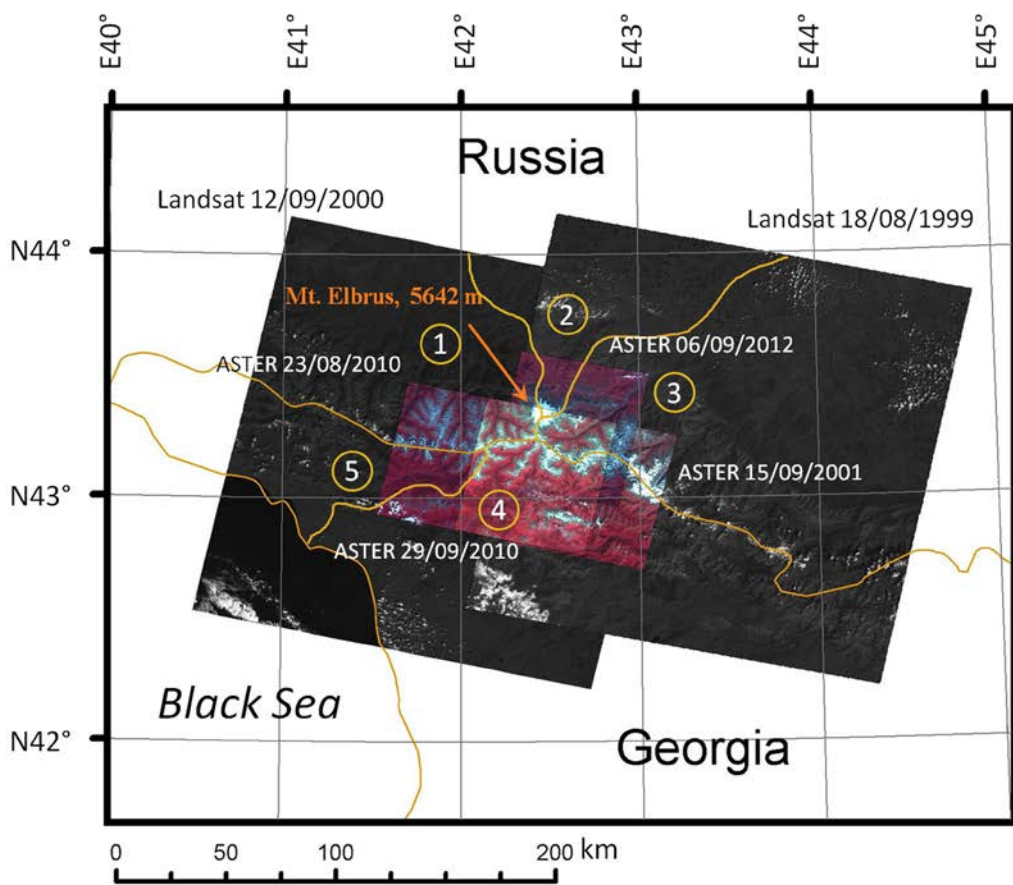
663 Figure 4. Changes in glacierised area of Mt. Elbrus between 1999 and 2012. See Table 4 for the
664 statistics of changes in areas of individual glaciers. The 1999 Landsat ETM+ image (Table 1) is
665 used as background.

666 Figure 5. Expansion of exposed rocks on the southern slope of Mt. Elbrus: (a) 1999 and (b) 2012.
667 Arrows point at the expanded areas of exposed rocks. The 1999 Landsat ETM+ image (Table
668 1) is used as background.

669 Figure 6. (a) JJA temperature and (b) October-April precipitation for Abastumani, Klukhorskyi
670 Pereval and Terskol stations. Horizontal lines show record averages for each station.

671 Figure 7. Cumulative mass balance of Garabashi and Djankuat glaciers (WGMS, 2013;
672 unpublished records from the Institute of Geography, Russian Academy of Science for
673 Garabashi in 2012).

674



675

676 Figure 1. Study area and satellite imagery used for the analysis. The yellow lines show the Black
 677 Sea coastline, the MCR, and the catchment boundaries. The catchments are numbered as
 678 follows: (1) Kuban; (2) Malka; (3) Baksan; (4) Inguri; and (5) Kodori.

679

680



683 Figure 2. Oblique aerial photograph of (a) glaciers on Mt. Elbrus and (b) snout of the Malyi
684 Azau glacier. Note the clearly defined glacier boundaries and a very limited extent of debris
685 cover. Photograph by I.I. Lavrentiev (25 August 2009).

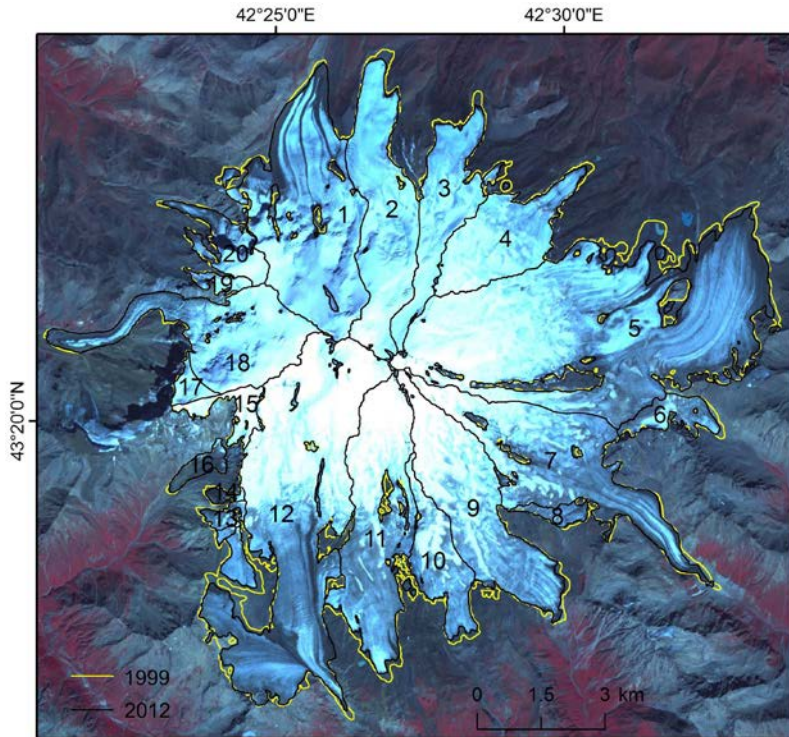
686



687

688 Figure 3. Oblique aerial photograph of the Donguz-Orun glacier which has the highest extent of
689 debris cover in the sample. Photograph by I.I. Lavrentiev (25 August 2009).

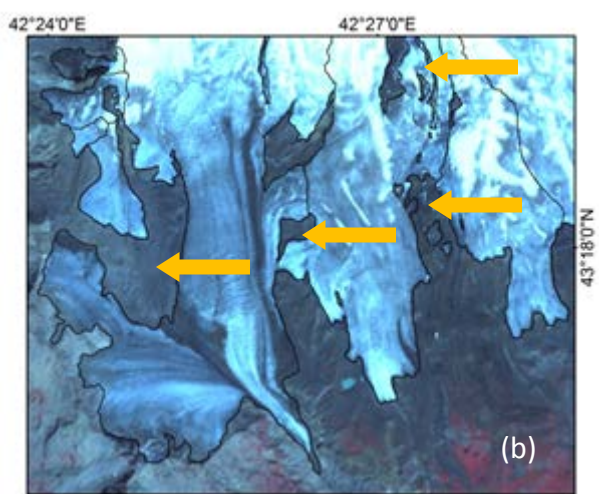
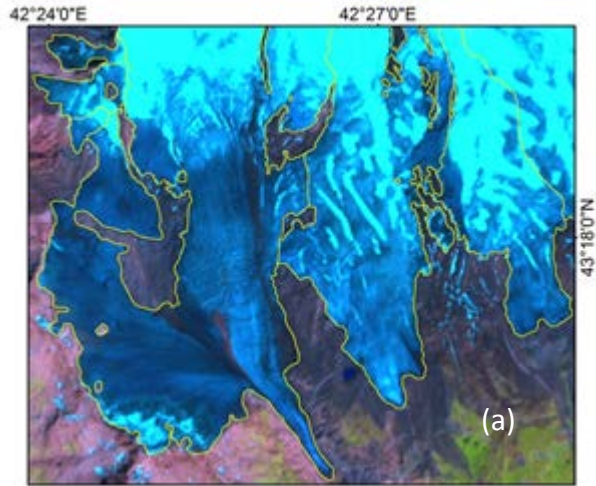
690



691

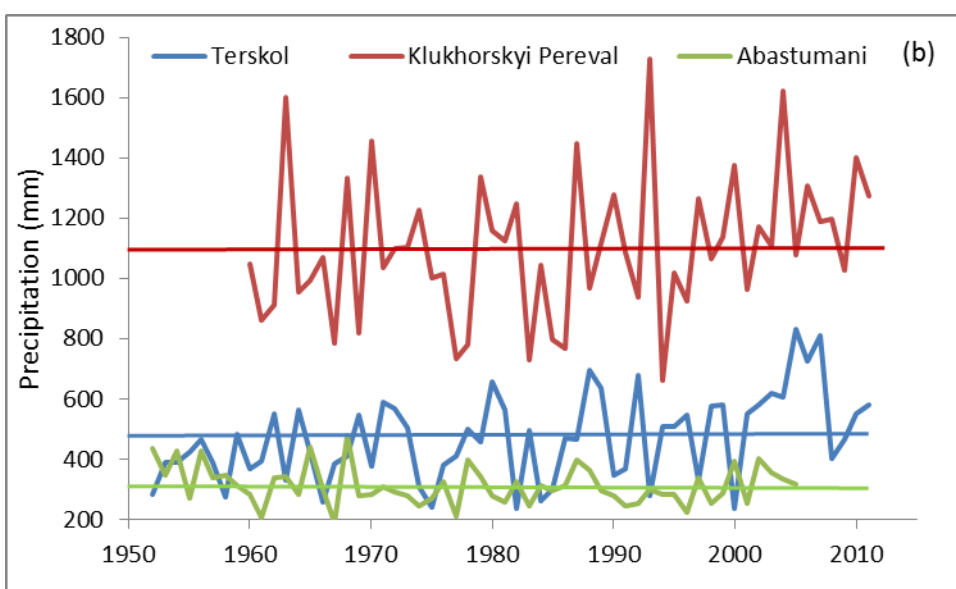
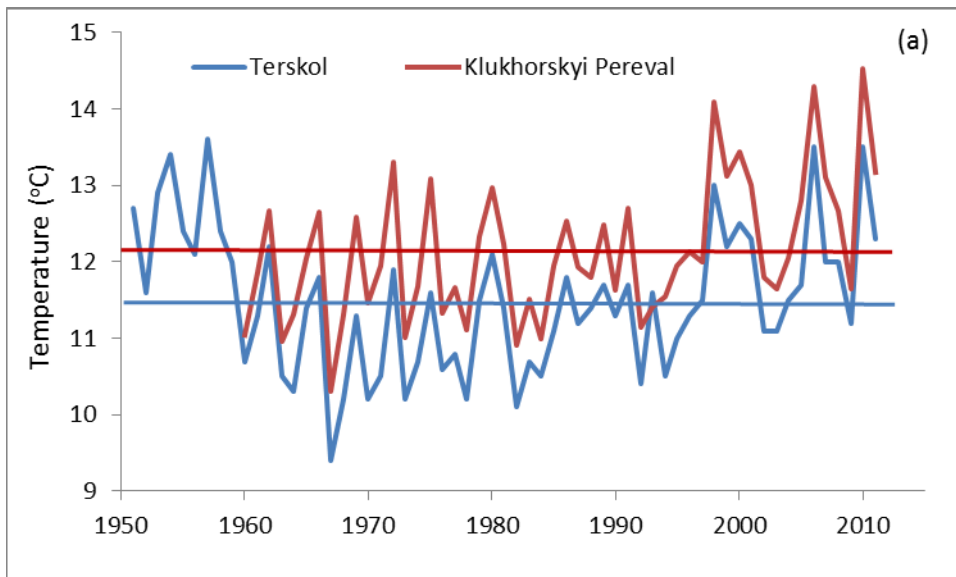
692 Figure 4. Changes in glacierised area of Mt. Elbrus between 1999 and 2012. See Table 4 for the
693 statistics of changes in areas of individual glaciers. The 1999 Landsat ETM+ image (Table 1) is
694 used as background.

695



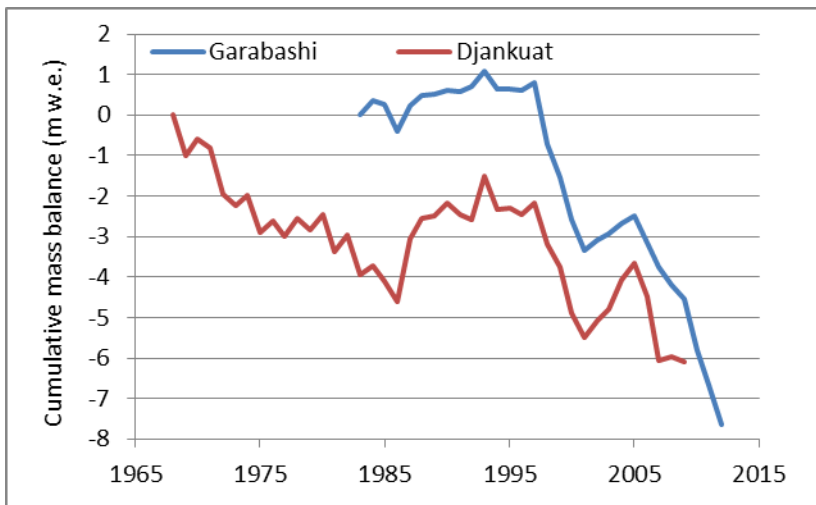
699 Figure 5. Expansion of exposed rocks on the southern slope of Mt. Elbrus: (a) 1999 and (b) 2012.
700 Arrows point at the expanded areas of exposed rocks. The 1999 Landsat ETM+ image (Table
701 1) is used as background.

702



705 Figure 6. (a) JJA temperature and (b) October-April precipitation for Abastumani, Klukhorskyi
 706 Pereval and Terskol stations. Horizontal lines show record averages for each station.

707



708

709 Figure 7. Cumulative mass balance of Garabashi and Djankuat glaciers (WGMS, 2013;
710 unpublished records from the Institute of Geography, Russian Academy of Science for
711 Garabashi in 2012).

712

713

714